Current Drug Delivery, 2018, *15*, 1449-1458

RESEARCH ARTICLE

The Influence of Microneedles on the Percutaneous Penetration of Selected Antihypertensive Agents: Diltiazem Hydrochloride and Perindopril Erbumine

Emmy Luu[1], Kevin B. Ita[1,*], Matthew J. Morra[2] and Inna E. Popova[2]

[1]*College of Pharmacy, Touro University California, Mare Island-Vallejo, CA, USA;* [2] *Department of Soil and Water Systems, University of Idaho, Moscow, Idaho, ID 83844-2339, USA*

ARTICLE HISTORY

Received: March 05, 2018
Revised: May 15, 2018
Accepted: July 23, 2018

DOI:
10.2174/1567201815666180730125941

Abstract: ***Background:*** It is well documented in the scientific literature that high blood pressure can lead to cardiovascular disease. Untreated hypertension has clinical consequences such as coronary artery disease, stroke or kidney failure. Diltiazem hydrochloride (DH), a calcium-channel blocker, and perindopril erbumine (PE), an inhibitor of the angiotensin converting enzyme are used for the management of hypertension.

Objective: This project will examine the effect of microneedle rollers on the transport of DH and PE across pig ear skin. The use of the transcutaneous route of administration reduces and in sometimes eliminates the trauma and pain associated with injections. Furthermore, there is increased patient compliance. The purpose of this project was to study the effect of stainless steel microneedles on the transdermal delivery of DH and PE.

Method: We utilized vertical Franz diffusion cells to study *in vitro* transport of DH and PE across microneedle-treated pig ear skin. Confocal laser scanning microscopy (CLSM) was used to characterize microchannel depth. Transdermal flux values were determined from the slope of the linear portion of the cumulative amount *versus* time curve.

Results: There was a 113.59-fold increase in the transdermal permeation of DH following the application of microneedle roller compared to passive diffusion.

Conclusion: In the case of PE, there was an 11.99-fold increase in the drug transport across pig skin following the application of microneedle rollers in comparison with passive diffusion. Student's t-test and Mann-Whitney's rank sum test were used to determine statistically significant differences between experimental and control groups.

Keywords: Hypertension, diltiazem hydrochloride, perindopril erbumine, transdermal drug delivery, microneedles, skin.

1. INTRODUCTION

Every year, 614,348 people die from Cardiovascular Disease (CVD) in the United States of America [1]. There is a considerable body of scientific evidence showing that high blood pressure can cause CVD [2]. Approximately, 78 million adults who are ≥20 years old suffer from hypertension in the United States [3, 4]. According to the Joint National Committee (JNC 8) on the prevention, detection, evaluation, and treatment of high blood pressure, this pathological disorder is characterized by elevated systolic blood pressure (SBP) (>140 mmHg) and diastolic blood pressure (>90 mmHg) [5]. According to the 2014 heart disease and stroke statistics, 82% of hypertensive Americans are aware of this disorder and 75% takes antihypertensive medications; however, high blood pressure is controlled in only 53% of those with hypertension [4]. It is challenging for patients to comply with their therapeutic regimens using traditional dosage forms such as tablets, capsules, and injections [6]. Most pediatric patients who have hypertension struggle to swallow tablets and have an adverse reaction to needles or injections [7]. Percutaneous drug transport addresses the limitations associated with oral and parenteral drug administration [8]. Oral drug delivery can lead to drug degradation in the stomach, gastric irritation, and presystemic drug metabolism [9]. It has been demonstrated that the transdermal route can be used to increase bioavailability [10]. In addition, the percutaneous route of drug administration is also advantageous when compared with hypodermic injections. The later produces medical waste and increases the risk of disease transmission, especially in developing countries where reusing needles is a common practice [11]. Furthermore, transdermal drug delivery systems is non-invasive, inexpensive and can be self-administered [11].

Most antihypertensive medications are administered to patients as tablets; however, tablets have drawbacks such as gastric irritation, erratic absorption, and first pass effect [12]. Transdermal drug administration avoids the limitations of the oral and injectable routes [9]. It is particularly useful for low dosage and potent compounds with optimal physiochemical properties [13]. Only few medications can cross the human

*Address correspondence to this author at the College of Pharmacy, Touro University, Mare Island-Vallejo, California, CA 94592, USA;
E-mail: kevin.ita@tu.edu

1875-5704/18 $58.00+.00 © 2018 Bentham Science Publishers

Current Drug Delivery

skin in therapeutic quantities [14]. The outermost layer of the epidermis (stratum corneum), hinders the quantity of medications which can enter the systemic circulation through the skin [9, 15]. The human skin comprises three layers- the epidermis, dermis and subcutaneous layer [16]. The SC is 10 to 20 μm thick and is composed of corneocytes (CCs) embedded in intercellular lipids [9, 14]. The corneocytes form the "bricks", while the lipids form the "mortar" [9, 17]. CCs are flat anucleated cells with keratin filaments as well as filaggrin [18, 19]. These cells are embedded in a lipid matrix consisting mainly of ceramides, cholesterols and free fatty acids [18, 20]. Beneath the SC is the Viable Epidermis (VE), which is made up of the stratum granulosum, stratum basale and stratum lucidum [21-23]. The VE is 50 to 100 μm thick [24]. The thickest component of the skin is the dermis, which is 4 mm in depth [24]. Several techniques are available for transdermal drug delivery enhancement. These include sonophoresis [25], iontophoresis [26] and microneedles [27].

The past few decades have witnessed a rapid increase and maturation of microfabrication and nanofabrication technologies [28, 29]. Nanoarchitectonic principles have been used to develop smart devices with advanced functions in the fields of biology and medicine [28]. The tools for constructing nanoarchitectonics include regulated atomic/molecular manipulation, chemistry-based molecular modification, controlled physicochemical interactions, self-assembly and self-organization [28]. One of the many challenges faced by drug delivery scientists is the creation of materials with precisely controlled surface and/or bulk microstructures. Researchers are now able to create unique micro- and nanostructures by utilizing technologies such as photolithography and etching [30]. Microneedles (MNs) are micron-sized needles(less than 1000μm) which can pierce the SC and facilitate transdermal drug delivery [31]. They are of the optimal length, long enough to pierce into the skin and short enough to avoid causing pain for patients [9]. The use of MNs is advantageous in comparison with injections or passive transdermal patches [32]. It has been demonstrated that microneedles can penetrate the stratum corneum effectively in a pain-free manner, and may therefore be a promising approach for drug administration [33]. There are five classes of MNs- solid, dissolving, hollow, coated and hydrogel-forming [12, 34]. The MNs are made from mechanically robust materials such as stainless steel [35, 36] or water-soluble materials loaded with medications [37, 38]. These medications are released into the skin following administration [39]. One of the benefits of solid microneedles is that they are strong enough to penetrate the skin [39]. MNs have benefits and limitations [33, 40]. MNs made from biodegradable materials may be too weak to pierce the epidermis [41]. Hollow microneedles can be fabricated in tandem with microfluidic components [42]. Microfluidic devices enable fluids to be manipulated within architectures on the size scale of micrometers [43]. These devices are typically designed to ensure levels of precision not possible with conventional macroscale approaches [43]. Silicon hollow microneedle based microfluidic devices have also been developed for transdermal drug delivery applications [42]. Most MNs create micrometer-sized pores in the skin, which increases transdermal drug delivery rates [44]. MNs are minimally invasive, easy to dispose and can increase transcutaneous flux values for medications [45]. MNs should be robust so that the skin can be pierced without causing any bleeding [46].

MNs can be created out of water soluble or biodegradable polymer which encapsulates the drug within the microneedle matrix [39]. Ideally, the MNs can dissolve or degrade into the skin, which releases the encapsulated drug payload and prevents sharp waste [39]. Many studies have shown that the use of microneedle patches can be challenging especially on large areas of the skin due to skin deformation. MN rollers overcome this challenge by creating micron-sized pores across the skin. These pores are permeable to small-molecule drugs and proteins [41]. Once the MNs are rolled on the skin, a single microneedle pierces the skin numerous times [41]. Despite the increased drug permeation, a microneedle roller (Fig. **1**) also has limitations: the misuse of this device may cause overdose, potential injury, and contamination of the skin [41, 47, 48]. In addition, the microneedle tips could break and act as biohazardous waste [48]. Furthermore, dosage accuracy could become more difficult to measure when compared to hypodermic needles [12]. Currently, neither microneedles nor microneedle rollers are available for clinical use [49]. However, a microneedle patch loaded with an inactivated influenza vaccine is currently undergoing clinical trials [50]. In this project, we examined the influence of microneedle rollers on the transdermal permeation of two antihypertensive drugs- diltiazem hydrochloride (DH) and perindopril erbumine (PE).

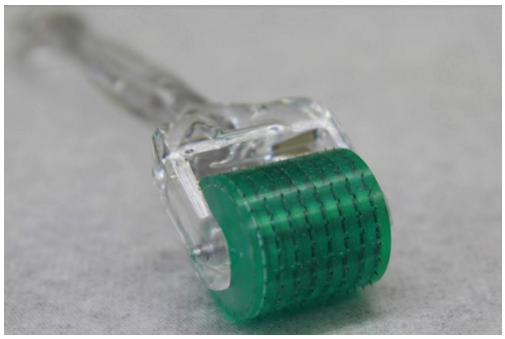

Fig. (1). Microneedle roller.

Diltiazem hydrochloride, [(2S,3S)-5- [2-(dimethylamino) ethyl]-2-(4-methoxyphenyl)-4-oxo-2,3-dihydro-1,5-benzothiazepin-3-yl] acetate; hydrochloride (Fig. **2a**), is a benzothiazepine derivative which is used in the clinic for the management of hypertension [51]. The chemical structure of DH is shown in Fig. (**1**). The drug inhibits transmembrane influx of calcium ions into myocardial cells such as the vascular smooth muscle, leading to dilation of the coronary arteries and a decrease in myocardial contractility [51]. In addition, DH enables the heart to pump blood at a normal rate by relaxing its blood vessels as well as increasing oxygen and blood flow to the heart [52]. DH has a molecular weight of 450.978 g/mol with a short half-life (3 to 4.5 hours), which requires frequent dosing. Frequent dosing may reduce patient compliance [53]. A transdermal microneedle approach may be useful for the transdermal delivery of DH. Perindopril erbumine, ((2S,3aS,7aS)-1- [(2S)-2- [[(2S)-1-ethoxy-1-oxopentan-2-yl] amino] propanoyl] 2,3,3a,4,5,6,7,7a-octahydroindole-2-carboxylic acid) (Fig. **2b**), is an angiotensin-converting enzyme (ACE) inhibitor, which is used for the

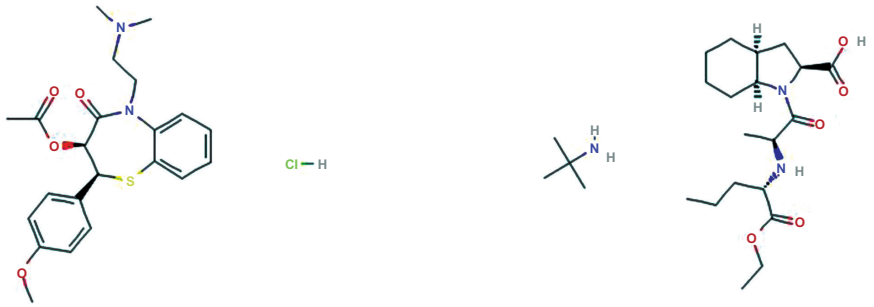

(a) Chemical Structure of Diltiazem Hydrochloride (DH)

(b) Chemical Structure of Perindopril Erbumine (PE)

Figs. (2). Chemical structures of (**a**) Diltiazem Hydrochloride and (**b**) Perindopril Erbumine.

management of hypertension and heart failure [54]. The chemical structure of PE is shown in Fig. (**2b**). PE has a short biological half-life of 1 to 3 hours [55] and a molecular weight of 441.613 g/mol. It acts by inhibiting the renin-angiotensin system through the prevention of the conversion of angiotensin I to angiotensin II [54]. The biotransformation of perindopril to perindoprilat, the active metabolite, is approximately 20% [3].

Our hypothesis is that the microneedles can significantly increase the percutaneous transport of DH and PE across pig ear skin. The ease of application and cost effectiveness of the transdermal route make it an attractive approach for drug delivery. To date, no study has been carried out on microneedle-mediated transdermal delivery of DH and PE. The aim of this project was to examine the effect of microneedle rollers on the transport of selected antihypertensive agents across pig ear skin.

2. MATERIALS AND METHODS

2.1. Materials

Diltiazem hydrochloride (DH), perindopril erbumine (PE) and 0.1M isotonic Phosphate Buffer Saline (PBS) were bought from Sigma Aldrich (St. Louis, MO, USA). Distilled de-ionized water was obtained from NanoPure Infinity Ultrapure water purification system (Barnstead, Dubuque, IA, USA). Stainless steel microneedle rollers (0.5mm) were bought from Pearl Enterprises LLC (Lakewood, New Jersey, USA). Electric hair clipper was purchased from Walgreens, a local pharmacy store (Vallejo, CA). Electric dermatome was purchased from Nouvag® (Goldach, Switzerland). Franz diffusion system (PermeGear, Hellertown, PA, USA) was used for experiments. Frozen porcine ears were purchased from Pel-Freez Arkansas LLC (Rogers, Arkansas, USA). DH and PE were reconstituted in only PBS prior to experiments.

2.2. Methods

2.2.1. Skin Preparation

The Institutional Biosafety Committee (IBC) of Touro University California (Mare Island-Vallejo, CA, USA) approved the experiments. Pig ears were shaved with an electric hair clipper and sliced with a dermatome [56] to 550µm. Split-thickness skin samples were wrapped with aluminum foil and stored at the temperature of -20°C. Before diffusion studies, split-thickness skins were left to thaw to room temperature (approximately 25°C). Each skin sample was then measured three times with a Digimatic micrometer (Mitutoyo, Tokyo, Japan) to determine its average thickness.

2.2.2. Diffusion of DH and PE Across Pig Skin In vitro

The permeability of each drug (DH or PE) across pig skin (the thickness was 550µm) was evaluated *in vitro*, using vertical Franz diffusion cells (PermeGear, Hellertown, PA, USA). The volume of the receptor compartment was 12 mL while the diffusion area was 1.77 cm^2. High-vacuum grease (Dow Corning, Midland, MA, USA) was applied on the receptor compartment, which was secured with a metal clamp to prevent loss of drug solution through lateral diffusion [35]. Stainless steel microneedle rollers were used to create microchannels in porcine ear skin. The microneedle roller was applied to the porcine ear skin 15 times in an asterisk-like direction (five times horizontally, vertically, and diagonally) [35]. The roller was applied with a force of 15 lbs (determined with a weighing balance) for 1 minute. Split-Thickness Skin (STS) samples (550µm) were first treated with microneedle rollers and then used for the experiments while untreated STS samples served as the controls.

The pig skin samples (pre-treated and control) were mounted on the Franz diffusion cells and the experiments were conducted at 37 °C. There were six experiments each for diltiazem hydrochloride and perindopril erbumine (n=6). In each set of experiments, 1 mL of diltiazem hydrochloride (~2940 mg/mL) or 1 mL of perindopril erbumine (~70 mg/mL) were utilized. The formulation of both drugs used in this study is presented in Table **1**. During the experiments, the donor compartment and sampling port were covered with parafilm® and aluminum foil to prevent evaporation. Essentially, 1mL of receptor buffer (PBS pH 7.4) was withdrawn from the receptor compartment every 2 hours for 12 hours and an equal volume of fresh PBS was used to replace the withdrawn fluid. The two drugs (DH and PE) were assayed using Liquid Chromatography-Mass Spectrometry Analysis (LC-MS).

2.2.3. Determination of DH and PE by LC-MS

The system utilized for LC-MS consisted of an Agilent 1200 Series HPLC equipment linked to an Agilent G1969A TOF-MS system equipped with an electrospray ionization

(ESI) source (Agilent, Santa Clara, CA, USA). We employed a reverse-phase Agilent Zorbax Eclipse Plus C18 (100 mm × 2.1 mm, 3.5 microns) analytical column, protected with a guard column (12.5 mm × 4.6 mm, 5 microns) for analysis. The injection volume was 5 µL. The mobile phase comprising 0.1% formic acid in water (solvent A) and 0.1% formic acid in methanol (solvent B) was used for chromatography. A linear gradient from 15% to 95% B was implemented in 7 minutes while isocratic elution was carried out for 2 minutes with 95% of solvent B. A final equilibrium was achieved with 15% of solvent B for 5 minutes. The flow was diverted from the MS for the first 3 minutes of the analysis to avoid MS contamination and ion suppression. The flow rate was at 0.3 mL per minute. Nebulizer gas temperature, nebulizer pressure and drying gas (N2) flow rate were 350°C, 2.4 x 10^5 Pa and 12 liters per minute respectively. Mass spectrometry was conducted in the positive electrospray ionization mode (ESI MS/MS). The absolute values for electrospray ionization potential and collision-induced dissociation potential were 3500 V and 175 V respectively. Compounds were analyzed in the positive ESI MS/MS mode by quantifying the specific product ion. LC-MS was performed in a profile mode with an m/z ranging from 90 to 500 atomic mass units. A mass analysis standard was used for assay in the reconstructed ion current mode using the m/z of 415.17 for diltiazem and 369.24 for perindopril.

2.2.4. Confocal Laser Scanning Microscopy

Confocal Laser Scanning Microscope (CLSM) was used to characterize the depth of the created microchannels. Excised split thickness porcine ear skin was treated with microneedles while untreated pig skin samples served as the controls. We applied 20 µL of the fluorescent dye AlexaFluor 633 (Life Technologies, Eugene, OR, USA) to the porated skin samples for approximately 2 minutes. A spatula was then used to apply the dye over the microneedle-treated skin to ensure evenly distribution. Excess AlexaFluor 633 was removed with kimwipes®. Pig ear skin samples, pretreated with microneedles, were sliced into 2 to 3 strips and mounted onto a Tissue-Tek Cryomold (Sakura Finetek Inc., Torrance, CA, USA). The control skin samples had the same protocol, but without the use of microneedles. Skin samples were covered with optimum cutting temperature (OCT) embedding medium and stored in the -80°C freezer until it was ready for use. Cryosectioning was performed using a Leica CM1950 Cryostat (Leica Biosystems, Buffalo Grove, IL, USA). Skin samples measuring 10 µm thick were obtained following cryosectioning. These samples were placed on labeled glass slides and their transmission images were captured with a Leica TCS LSI laser scanning confocal microscope at 5x magnification. Excitation was at 631 nm while emission was at 647 nm. X-Z sectioning was carried out to identify the depth of fluorescent dye penetration. The frame size was fixed at 1024 by 1024 pixels. Gain (blue) and offset (green) were used to increase image contrast.

2.2.5. Data Analysis

Steady-state transdermal flux values were calculated from the linear portion of the mean cumulative amount *versus* time curves (n=6). Equation (1) was used to account or dilution as documented by Hayton and Chen [57]:

$$C_n^1 = C_n\left(\frac{V_T}{V_T - V_S}\right)\left(\frac{C_{n-1}^1}{C_{n-1}}\right) \quad (1)$$

In the equation, C_n^1 is the corrected concentration, C_n is the measured concentration in the nth sample, V_s is the total volume of the receiver fluid (12mL) and V_s is the volume of sample withdrawn from the receiver fluid (1mL). Both C_{n-1}^1 and C_{n-1} are the corrected and measured concentration, respectively, in the (n-1)th sample.

The cumulative amount *versus* time curve was also fitted to the appropriate solution (Equation 2) [58-60] of the non-steady-state diffusion equation (Fick's second law), with the following boundary conditions: (a) that there is no depletion of the drug in the donor compartment throughout the experiment, (b) that the receptor compartment provides "sink conditions", and (c) that at t = 0, there is no drug in the skin ([61]):

$$Q(t) = AKhC\left[D\frac{t}{h^2} - \frac{1}{6} - \frac{2}{\pi^2}\sum_{n=1}^{\infty}\frac{(-1)^n}{n^2}\exp\left(\frac{-Dn^2\pi^2 t}{h^2}\right)\right] \quad (2)$$

where Q(t) is the amount that passes through the membrane and reaches the receptor solution at a given time (t), A is the surface diffusion area, K is the partition coefficient of the permeant between the membrane and the donor vehicle, h represents the thickness of the membrane, D is the diffusion coefficient of the permeant across the membrane and C represents the concentration of the permeant in the donor solution, which in this study is the solubility of the drug in the vehicle. Prism, Version 7 (GraphPad Software, Inc La Jolla, CA, USA) was used for the fitting procedure while the drug's partitioning (*kh*) and diffusivity $\left(\frac{D}{h^2}\right)$ parameters were used to estimate the permeability coefficient, *kp*:

$$Kp = (Kh) * \left(\frac{D}{h^2}\right) = \frac{KD}{h} \quad (3)$$

The steady-state flux was subsequently calculated:

$$Jss = Kp * C \quad (4)$$

and the results compared to the experimentally derived data (Tables **1** and **2**).

2.2.6. Statistical Analysis

Statistical analysis was performed using GraphPad Prism 7 (GraphPad Software, Inc. La Jolla, Ca, USA). The Student's t-test and the Mann-Whitney rank sum test were executed to determine statistical significance. The Student's t-test was used for perindopril erbumine due to its normal distribution (parametric) while the Mann-Whitney rank sum test was used for diltiazem hydrochloride due to its skewed distribution (non-parametric). Statistical significance was set at A p-value of <0.05. The mean of replicate measurements (n=6) with corresponding standard deviation was used to plot linear and bar graphs.

3. RESULTS

3.1. Characterization of Microneedle Roller

We studied the effect of a stainless steel microneedle roller on the transcutaneous diffusion of selected antihyper-

tensive agents (diltiazem hydrochloride and perindopril erbumine) across porcine ear skin (the thickness was 550µm). Each microneedle roller has microneedles protruding from a cylindrical surface area. The needles are 500 µm long with a density of 192 (Fig. **1**).

3.2. Confocal Laser Scanning Microscope (CLSM)

CLSM was used to determine microchannel depth at 5x. AlexaFluor 633 dye was used on each skin sample to investigate the microchannel created following the application of microneedle rollers. A single microchannel measuring 132±1.6 µm deep is shown in Fig. (**3B**). The microchannel, created following the breach of the SC by microneedles can be seen on the image. In contrast, there is no microchannel in the image of the control sample (Fig. **3A**).

3.3. *In vitro* Diffusion Studies

The cumulative amount of DH transported across untreated and microneedle-treated pig ear skin over 12 hours is shown in Fig. (**4A**). The corresponding DH flux values(microneedle-assisted and control) are shown in Fig. (**4B**). A similar time (12 hours) has previously been used in transdermal drug delivery experiments by Burger *et al.* [62]. There was a 113.59-fold increase in the transdermal permeation of DH following the application of microneedle roller (788.34 ± 212.85 µg/cm^2/hr) compared to passive diffusion (6.94 ± 1.87 µg/cm^2/hr). The cumulative amount of PE, which permeated across untreated porcine ear skin and microneedle-treated porcine ear skin over 12 hours, is shown in Fig. (**5A**). The corresponding PE flux values(microneedle-assisted and control) are shown in Fig. (**5B**). It can be seen that the use of microneedle roller resulted in an 11.99-fold increase in the amount of PE which diffused across porcine skin (1271.7 ± 211.95 µg/cm^2/hr) versus passive diffusion (105.98 ± 61.47 µg/cm^2/hr). The transdermal flux values for DH and PE across microneedle-treated pig skin in comparison with passive penetration are also shown in Table **1** while the results of curve fitting of data to the solution of Fick's second law are shown in Table **2**. The results obtained though curve-fitting were of the same order of magnitude in comparison with experimentally derived values.

4. DISCUSSION

This project focused on the influence of microneedle rollers on the transdermal flux values of DH and PE across porcine ear skin. Our results from the diffusion studies indicate that transdermal flux values increased significantly for microneedle-treated skin when compared to untreated microneedle porcine ear skin. Data from our present study indicate that a microneedle roller is efficient at enhancing the *in vitro* trans-

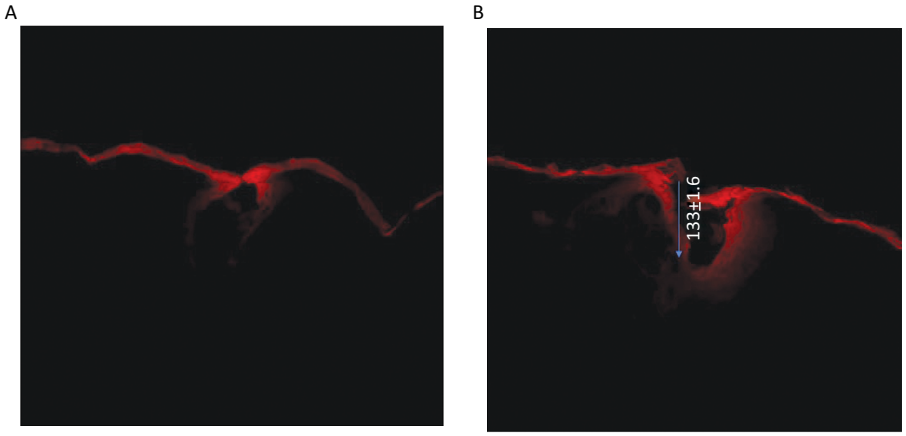

Fig. (3). Confocal laser scanning images made with AlexaFluor 633 on (**A**) untreated porcine ear skin and (**B**) microneedle-treated porcine ear skin at 5x magnification. The single microchannel of microneedle-treated porcine ear skin has a depth of 133± 1.6 µm (n=6).

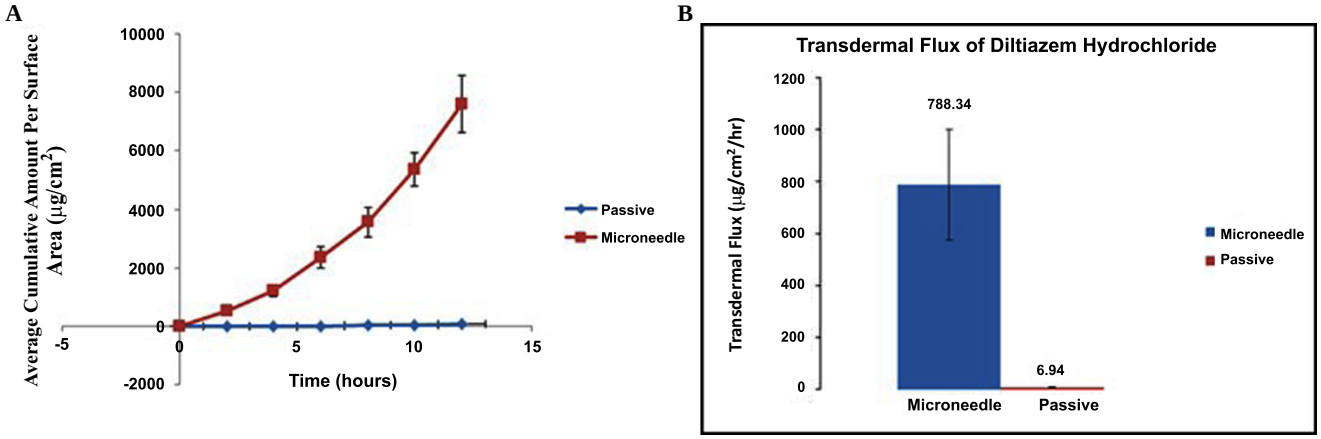

Fig. (4). Average cumulative amount *versus* time curve (**A**) and transdermal flux (**B**) of diltiazem hydrochloride across untreated and microneedle-treated porcine ear skin over 12 hours.

Table 1. Experimentally determined transdermal flux values (μg/cm^2/hr ± SD) of diltiazem hydrochloride and perindopril erbumine following treatment with a 500 μm microneedle roller. Untreated porcine skin samples served as controls(passive) (n=6).

Drug Name	Passive (μg/cm^2/hr)	Microneedle (μg/cm^2/hr)	Enhancement Ratio	p-value
Diltiazem Hydrochloride	6.94 ± 1.87	788.34 ± 212.85	113.59	0.018
Perindopril Erbumine	105.98 ± 61.47	1271.7 ± 211.95	11.99	0.0075

Table 2. Transdermal flux values (μg/cm^2/hr ± SD) of diltiazem hydrochloride and perindopril erbumine derived from curve-fitting (the solution to Fick's second law).

Drug Name	Passive (μg/cm^2/hr)	Microneedle (μg/cm^2/hr)	Enhancement ratio	p-value
Diltiazem Hydrochloride	6.32 ± 3.04	711.04 ± 159	112.5	<0.05
Perindopril Erbumine	110.95 ± 25.2	1331.41± 238	12.1	<0.05

port of DH and PE. The evidence from this current study further supports the hypothesis that the application of microneedles on porcine ear skin can significantly increase transcutaneous flux. Porcine ear skin samples were used for this study because it shares anatomical similarities with the human skin [63]. Diltiazem hydrochloride is a calcium channel blocker utilized for the management of hypertension [64, 65]. The drug undergoes extensive presystemic metabolism following absorption leading to a reduced drug bioavailability (30 to 40%) [66]. Complex biotransformation (N-demethylation, O-demethylation and deacetylation) has been observed for DH [67]. In addition, the drug causes GI disturbances, including nausea, vomiting and constipation following oral ingestion [64]. These properties provide strong impetus for the development of a DH-loaded transdermal formulation [67].

Several percutaneous delivery enhancement techniques for diltiazem hydrochloride have been published [65, 67-70]. Gupta and Mukherjee investigated the influence of different ratios of polymers, ethylcellulose (EC), and povidone (PVP) on the transdermal delivery of DH across depilated freshly excised abdominal mouse skin [65]. It was found that the optimal transdermal drug delivery system for DH comprised films prepared from povidone:ethylcellulose (1:2) [61]. The authors showed that the cumulative amount of the drug transported across mouse skin was proportional to the square root of time (Higuchi kinetics) [65]. Higuchi equation shows a direct proportionality between the cumulative amount of drug released and the square root of time [71]. Fu and Kao have also demonstrated that Higuchi drug release can be Fickian [72]. Fickian diffusion occurs mostly in polymeric systems when the temperature is well above the glass transition temperature (Tg) and this type of diffusion features a solvent diffusion rate, R_{diff}, slower than the polymer relaxation rate, R_{relax} ($R_{diff} < R_{relax}$) [73]. In this instance, the polymer is in the rubbery state and its chains present a higher mobility which allows an easier penetration of the solvent [73]. In contrast, zero-order drug release occurs when the dissolution of the polymer appears to control the drug release rate [74].

Ionic liquids are organic salts, comprising of a large and asymmetric organic cation and an organic or inorganic anion, that are liquid at or near room temperature [69]. They possess negligible vapor pressure, the ability to dissolve organic, inorganic and polymeric materials and a high thermal stability [69]. Recently, Monti and coworkers investigated the effect of several ionic liquids on the percutaneous transport and skin retention of diltiazem hydrochloride salt [DH] and the free base [DB] [69]. The authors studied the mono- and dicationic derivatives of 1,4-diazabicyclo [2.2.2]octane (DABCO), a dialkyl morpholinium salt and a Brønsted acidic ionic liquid and found a significant increase in transdermal flux values of DH and DB across rat skin following the use of all the ionic liquids [69]. Interestingly, N-dodecyldabco bromide was the best enhancer for both drug forms, even though a certain degree of toxicity was observed [69]. On the other hand, N-methyl-N-decylmorpholinium bromide displayed a good balance between enhancer activity and cytotoxicity [69]. In another study, Jain *et al*. used chitosan and other polymers to prepare different transdermal drug delivery systems (matrix and membrane-controlled) loaded with DH [75]. It was shown that DH release from the matrix systems was enhanced with increased hydrophilic polymer concentration [75]. It was also observed that the release of DH from the membrane systems decreased when the rate controlling membrane was crosslinked and when citric acid was added to the chitosan drug reservoir gel [75]. The authors concluded that effective therapeutic concentration levels can be achieved by both drug delivery systems [75]. Although several approaches for increasing the transdermal delivery of DH have been reported in the literature, this is the first time, to our knowledge, that microneedles are being investigated for the percutaneous transport of diltiazem hy-

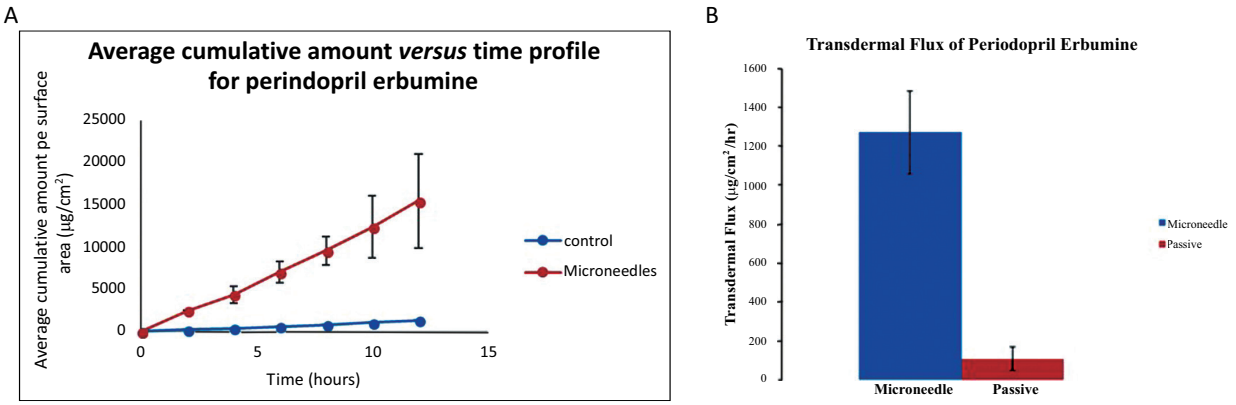

Fig. (5). Average cumulative amount *versus* time curve (**A**) and transdermal flux (**B**) of perindopril erbumine across untreated and microneedle-treated porcine ear skin over 12 hours.

drochloride (DH). The overarching goal of our project is to develop a transdermal delivery system for DH. Percutaneous transport can lead to better patient compliance, optimal pharmacokinetic profile (uniform plasma concentration) and decreased side effects [35]. Our project examined the influence of microneedle rollers on the transdermal delivery of DH. In Fig. (**4B**), it is observed that there is a 113.59-fold increase in the percutaneous penetration of DH following the application of microneedle roller (788.34 ± 212.85 µg/cm^2/hr) compared to passive diffusion (6.94 ± 1.87 µg/cm^2/hr).

Perindopril erbumine is a long-acting angiotensin-converting enzyme (ACE) inhibitor used for the management of hypertension [76]. The low dose (4mg) and short biological half-life of PE provide the rationale for the development of a transdermal drug delivery system [77]. Although Helal and Lane wrote an excellent review on the transdermal delivery of perindopril erbumine (and other ACE inhibitors) [77], only one experimental work addresses the transcutaneous transport of PE [78]. Kute and coworkers studied the transdermal permeation of PE from proniosomal gel and reported that proniosomal gel with T20:T60 in ratio of 900:100 showed the highest percentage of drug release (80.03%) over period of 24 hrs [78]. In addition, the cumulative amount of drug which penetrated through rat abdominal skin from this optimized formulation was 75.263% [78]. In the present study, we used stainless steel microneedle rollers to deliver PE across pig ear skin *in vitro*. There was a 11.99-fold increase in the PE permeation across porcine skin following the application of a microneedle roller (1271.7 ± 211.95 µg/cm^2/hr) versus passive diffusion (105.98 ± 61.47 µg/cm^2/hr) (Fig. **5B**).

The use of microneedles can lead to enhanced drug transport across the skin [79-81]. The delivered compounds may vary in size from small molecules to high molecular weight compounds such as proteins [82-84]. Stainless steel microneedles are mechanically robust and can painlessly pierce the skin [83, 85]. This is especially significant for patients with needle phobia [45]. Li *et al*. indicated that pain induced by microneedles of length 500 to 1500 µm is relatively low when compared to hypodermic needles [86]. Microneedles increase skin permeability by producing micron-scale pathways and can actively drive drugs into the skin [87]. It can also reduce the chance of infections and skin irritations [45]. With the purpose of microneedle technology becoming a clinical reality, many challenges must be overcome. Microneedles should possess sufficient mechanical strength to penetrate the skin without breaking before or during insertion [34]. In a 2001 paper, Barry observed that 51 out of 129 drug delivery candidate products which were under clinical evaluation at the time were for skin delivery [88]. Significantly, 30% of 77 candidate products in preclinical development were also transdermal or dermal drug delivery systems [88]. Transdermal delivery is widely acknowledged as a non-invasive method for drug administration [69]. This approach avoids first-pass metabolism, leads to better patient compliance, and enhances therapeutic action [69]. Currently, the transdermal route of administration is used to deliver about 20 active pharmaceutical ingredients [89] and it is important to use different technologies for transdermal drug delivery enhancement. Our project addresses this challenge by evaluating the effect of microneedle rollers.

CONCLUSION

We studied the effect of stainless steel microneedle rollers on the percutaneous transport of diltiazem hydrochloride and perindopril erbumine. There were statistically significant differences in flux values of both drugs across untreated and microneedle-treated porcine skins following the application of microneedle rollers. Our results demonstrate that microneedles may be beneficial for the skin permeation of diltiazem hydrochloride and perindopril erbumine. The microneedle approach can also be extended to drugs from other therapeutic groups.

ETHICS APPROVAL AND CONSENT TO PARTICIPATE

The Institutional Biosafety Committee (IBC) of Touro University California (Mare Island-Vallejo, CA, USA) approved the experiments.

HUMAN AND ANIMAL RIGHTS

No human were used in the basis of this research. The reported experiments in accordance with the standards set forth in the 8th Edition of Guide for the Care and Use of Laboratory Animals (http:// grants.nih.gov/grants/olaw/Guide-for-thecare-and-use-of-laboratory-animals.pdf) published by the

National Academy of Sciences, The National Academies Press, Washington DC, United States of America.

CONSENT FOR PUBLICATION

Not applicable.

CONFLICT OF INTEREST

The authors declare no conflict of interest, financial or otherwise.

ACKNOWLEDGEMENTS

We thank Patricia Edwards of the Cellular and Molecular Imaging Lab at UC Davis who performed confocal imaging and cryosectioning. This work was supported by Touro University California, Mare Island-Vallejo, California, USA.

REFERENCES

[1] https://www.cdc.gov/nchs/fastats/deaths.htm Accessed on June 29, Accessed on June 29, **2017**.

[2] Rosendorff, C. Treatment of hypertension in patients with coronary artery disease. a case-based summary of the 2015 AHA/ACC/ASH scientific statement. *Am. J. Med.*, **2016**, *129*(4), 372-378.

[3] Buis, L.; Hirzel, L.; Dawood, R.M.; Dawood, K.L.; Nichols, L.P.; Artinian, N.T.; Schwiebert, L.; Yarandi, H.N.; Roberson, D.N.; Plegue, M.A.; Mango, L.C.; Levy, P.D. Text messaging to improve hypertension medication adherence in african americans from primary care and emergency department settings: results from two randomized feasibility studies. *JMIR Mhealth Uhealth*, **2017**, *5*(2), p. e9.

[4] Go, A.S.; Mozaffarian, D.; Roger, V.L.; Benjamin, E.J.; Berry, J.D.; Blaha, M.J.; Dai, S.; Ford, E.S.; Fox, C.S.; Franco, S.; Fullerton, H.J.; Gillespie, C.; Hailpern, S.M.; Heit, J.A.; Howard, V.J.; Huffman, M.D.; Judd, S.E.; Kissela, B.M.; Kittner, S.J.; Lackland, D.T.; Lichtman, J.H.; Lisabeth, L.D.; Mackey, R.H.; Magid, D.J.; Marcus, G.M.; Marelli, A.; Matchar, D.B.; McGuire, D.K.; Mohler, E.R. 3rd; Moy, C.S.; Mussolino, M.E.; Neumar, R.W.; Nichol, G.; Pandey, D.K.; Paynter, N.P.; Reeves, M.J.; Sorlie, P.D.; Stein, J.; Towfighi, A.; Turan, T.N.; Virani, S.S.; Wong, N.D.; Woo, D.; Turner, M.B.; American Heart Association Statistics Committee and Stroke Statistics Subcommittee. Heart disease and stroke statistics--2014 update: a report from the American Heart Association. *Circulation*, **2014**, *129*(3), e28-e292.

[5] James, P.A.; Oparil, S.; Carter, B.L.; Cushman, W.C.; Dennison-Himmelfarb, C.; Handler, J.; Lackland, D.T.; LeFevre, M.L.; MacKenzie, T.D.; Ogedegbe, O.; Smith, S.C.; Svetkey, Jr., L.P.; Taler, S.J.; Townsend, R.R.; Wright, J.T.; Narva, Jr., A.S.; Ortiz, E. 2014 evidence-based guideline for the management of high blood pressure in adults: report from the panel members appointed to the Eighth Joint National Committee (JNC 8). *JAMA*, **2014**, *311*(5), 507-520.

[6] Jepps, O.G.; Dancik, Y.; Anissimov, Y.G.; Roberts, M.S. Modeling the human skin barrier--towards a better understanding of dermal absorption. *Adv. Drug Deliv. Rev.*, **2013**, *65*(2), 152-168.

[7] Baracco, R.; Kapur, G. Clinical utility of valsartan in the treatment of hypertension in children and adolescents. *Patient Prefer Adherence*, **2011**, *5*, 149-155.

[8] Alexander, A.; Dwivedi, S.; Ajazuddin, T.K.; Giri, S.; Saraf, S.; Tripathi, D.K. Approaches for breaking the barriers of drug permeation through transdermal drug delivery. *J. Control. Release*, 2012, *164*(1), 26-40.

[9] Nguyen, K.T.; Ita, K.; Parikh, I.P.; Bair, D.A. Transdermal delivery of captopril and metoprolol tartrate with microneedles. *Drug Deliv. Lett.*, **2014**, *4*, 236-243.

[10] Jhawat, V.C.S.; Kamboj, S.; Maggon, N. Transdermal drug delivery systems: Approaches and advancements in drug absorption through skin. *Inter. J. Pharm. Sci. Rev. Res.*, **2013**, *20*(1), 47-56.

[11] Bartosova, L.; Bajgar, J. Transdermal drug delivery *in vitro* using diffusion cells. *Curr. Med. Chem.*, **2012**, *19*(27), 4671-4677.

[12] Zhu, D.D.; Wang, Q.L.; Liu, X.B.; Guo, X.D. Rapidly separating microneedles for transdermal drug delivery. *Acta Biomater.*, **2016**, *41*, 312-319.

[13] Kwan, P.; Sills, G.J.; Brodie, M.J.; The mechanisms of action of commonly used antiepileptic drugs. *Pharmacol. Ther.*, **2001**, *90*(1), 21-34.

[14] Bouwstra, J.A.; Honeywell-Nguyen, P.L. Skin structure and mode of action of vesicles. *Adv. Drug Deliv. Rev.*, **2002**, *54*(Suppl 1), S41-55.

[15] Lane, M.E. Skin penetration enhancers. *Int. J. Pharm.*, **2013**, *447*(1-2), 12-21.

[16] Saini, N.; Bajaj, A. Recent trend on transdermal drug delivery system ad advancements in drug delivery through skin. *Inter. J. Res. Pharm. Biosci.*, **2014**, *4*, 5-14.

[17] Barry, B.W. Novel mechanisms and devices to enable successful transdermal drug delivery. *Eur. J. Pharm. Sci.*, **2001**, *14*(2), 101-114.

[18] Akiyama, M. Corneocyte lipid envelope (CLE), the key structure for skin barrier function and ichthyosis pathogenesis. *J. Dermatol. Sci.*, **2017**, *88*(1), 3-9.

[19] Venus, M.; Waterman, J.; McNab, I. Basic physiology of the skin. *Surgery*(*Oxford*), **2011**, *29*(10), 471-474.

[20] Pham, Q.D.; Björklund, S.; Engblom, J.; Topgaard, D.; Sparr, E. Chemical penetration enhancers in stratum corneum- Relation between molecular effects and barrier function. *J. Control. Release*, **2016**, *232*, 175-187.

[21] Schulz, R.; Yamamoto, K.; Klossek, A.; Flesch, R.; Honzke, S.; Rancan, F.; Vogt, A.; Blume-Peytavi, U.; Hedtrich, S.; Schafer-Korting, M.; Ruhl, E.; Netz, R.R. Data-based modeling of drug penetration relates human skin barrier function to the interplay of diffusivity and free-energy profiles. *Proc. Natl. Acad. Sci. U.S.A*, **2017**, *114*(14), 3631-3636.

[22] Zirra, A.M. The functional significance of the skin's stratum lucidum. *Morphol. Embryol .(Bucur)*, **1976**, *22*(1), 9-12.

[23] Simpson, C.L.; Patel, D.M.; Green, K.J. Deconstructing the skin: Cytoarchitectural determinants of epidermal morphogenesis. *Nat. Rev. Mol. Cell Biol.*, **2011**, *12*(9), 565-580.

[24] Ita, K. Transdermal delivery of drugs with microneedles-potential and challenges. *Pharmaceutics*, **2015**, *7*(3), 90-105.

[25] Seto, J.E.; Polat, B.E.; Lopez, R.F.; Blankschtein, D.; Langer, R. Effects of ultrasound and sodium lauryl sulfate on the transdermal delivery of hydrophilic permeants: Comparative *in vitro* studies with full-thickness and split-thickness pig and human skin. *J. Control. Release*, **2010**, *145*(1), 26-32.

[26] Abla, N.; Naik, A.; Guy, R.H.; Kalia, Y.N. Contributions of electromigration and electroosmosis to peptide iontophoresis across intact and impaired skin. *J. Control. Release*, **2005**, *108*(2-3), 319-330.

[27] Arya, J.; Henry, S.; Kalluri, H.; McAllister, D.V.; Pewin, W.P.; Prausnitz, M.R. Tolerability, usability and acceptability of dissolving microneedle patch administration in human subjects. *Biomaterials*, **2017**, *128*, 1-7.

[28] Komiyama, M.; Yoshimoto, K.; Sisido, M.; Ariga, K. Chemistry can make strict and fuzzy controls for bio-systems: DNA nanoarchitectonics and cell-macromolecular nanoarchitectonics. *Bull. Chem. Soc. Jpn.*, **2017**, *90*, 967-1004.

[29] Jiang, T.; Deng, M.; James, R.; Nair, L.S.; Laurencin, C.T. Micro- and nanofabrication of chitosan structures for regenerative engineering. *Acta Biomater.*, **2014**, *10*(4), 1632-1645.

[30] Sebastien Henry, D.V.M.; Mark, G.; Allen, M.; Prausnitz, R. Microfabricated microneedles: A novel approach to transdemal drug delivery. *J. Pharm. Sci.*, **1998**, *87*(8), 922-925.

[31] Kalluri, H.; Kolli, C.S.; Banga, A.K. Characterization of microchannels created by metal microneedles: Formation and closure. *AAPS J.*, **2011**, *13*(3), 473-481.

[32] Cai, B.; Xia, W.; Bredenberg, S.; Li, H.; Engqvist, H. Bioceramic microneedles with flexible and self-swelling substrate. *Eur. J. Pharm. Biopharm.*, **2015**, *94*, 404-410.

[33] Ita, K.B. Transdermal drug delivery: Progress and challenges. *J. Drug Deliv. Sci. Technol.*, **2014**, *24*(3), 245-250.

[34] Olatunji, O.; Das, D.B.; Garland, M.J.; Belaid, L.; Donnelly, R.F. Influence of array interspacing on the force required for successful microneedle skin penetration: Theoretical and practical approaches. *J. Pharm. Sci.*, **2013**, *102*(4), 1209-1221.

[35] Hoang, M.T.; Ita, K.B.; Bair, D.A. Solid microneedles for transdermal delivery of amantadine hydrochloride and pramipexole dihydrochloride. *Pharmaceutics*, **2015**, *7*(4), 379-396.

[36] Rajabi, M.; Roxhed, N.; Shafagh, R.Z.; Haraldson, T.; Fischer, A.C.; Wijngaart, W.V.; Stemme, G.; Niklaus, F. Flexible and stretchable microneedle patches with integrated rigid stainless steel microneedles for transdermal biointerfacing. *PLoS One*, **2016**, *11*(12), e0166330.

[37] Quinn, H.L.; Bonham, L.; Hughes, C.M.; Donnelly, R.F. Design of a dissolving microneedle platform for transdermal delivery of a fixed-dose combination of cardiovascular drugs. *J. Pharm. Sci.*, **2015**, *104*(10), 3490-3500.

[38] Qiu, Y.; Li, C.; Zhang, S.; Yang, G.; He, M.; Gao, Y. Systemic delivery of artemether by dissolving microneedles. *Int. J. Pharm.*, **2016**, *508*(1-2), 1-9.

[39] Kim, Y.-C.; Park, J.-H.; Prausnitz, M.R.; Microneedles for drug and vaccine delivery. *Adv. Drug Deliv. Rev*., **2012**, *64*(14), 1547-1568.

[40] McCrudden, M.T.; Alkilani, A.Z.; McCrudden, C.M.; McAlister, E.; McCarthy, H.O.; Woolfson, A.D.; Donnelly, R.F. Design and physicochemical characterisation of novel dissolving polymeric microneedle arrays for transdermal delivery of high dose, low molecular weight drugs. *J. Control. Release*, **2014**, *180*, 71-80.

[41] Park, J.H.; Choi, S.O.; Seo, S.; Choy, Y.B.; Prausnitz, M.R. A microneedle roller for transdermal drug delivery. *Eur. J. Pharm. Biopharm*., **2010**, *76*(2), 282-289.

[42] Ashraf, M.W.; Tayyaba, S.; Nisar, A.; Afzulpurkar, N.; Bodhale, D.W.; Lomas, T.; Poyai, A.; Tuantranont, A. Design, fabrication and analysis of silicon hollow microneedles for transdermal drug delivery system for treatment of hemodynamic dysfunctions. *Cardiovasc. Eng*., **2010**, *10*(3), 91-108.

[43] Sun, Y.; Haglund, T.A.; Rogers, A.J.; Ghanim, A.F.; Sethu, P. Review: Microfluidics technologies for blood-based cancer liquid biopsies. *Anal. Chim. Acta*, **2018**, *1012*, 10-29.

[44] Ita, K. Transdermal delivery of heparin: Physical enhancement techniques. *Int. J. Pharm*., **2015**, *496*, 240-249.

[45] Kaur, M.; Ita, K.B.; Popova, I.E.; Parikh, S.J.; Bair, D.A. Microneedle-assisted delivery of verapamil hydrochloride and amlodipine besylate. *Eur. J. Pharm. Biopharm*., **2014**, *86*(2), 284-291.

[46] Kearney, M.C.; Brown, S.; McCrudden, M.T.; Brady, A.J.; Donnelly, R.F. Potential of microneedles in enhancing delivery of photosensitising agents for photodynamic therapy. *Photodiagnosis Photodyn. Ther*., **2014**, *11*(4), 459-466.

[47] Prausnitz, M.R. Microneedles for transdermal drug delivery. *Adv Drug Deliv. Rev*., **2004**, *56*(5), 581-587.

[48] Bariya, S.H.; Gohel, M.C.; Mehta, T.A.; Sharma, O.P. Microneedles: An emerging transdermal drug delivery system. *J. Pharm. Pharmacol*., **2012**, *64*(1), 11-29.

[49] Ita, K. Insights into the percutaneous penetration of antidiabetic agents. *J. Drug Target*, **2017**, *25*(2), 102-111.

[50] Luthy, K.E.; David, R.M.; Macintosh, J.L.B.; Eden, L.M.; Beckstrand, R.L. Attention-deficit hyperactivity disorder: Comparison of medication efficacy and cost. *J. Nurse Pract*., **2015**, *11*(2), 226-232.

[51] Ita, K. Recent trends in the transdermal delivery of therapeutic agents used for the management of neurodegenerative diseases. *J. Drug Target*, **2017**, *25*(5), 406-419.

[52] Ita, K. Percutaneous penetration of anticancer agents: Past, present and future. *Biomed. Pharmacother*., **2016**, *84*, 1428-1439.

[53] Karakatsani, M.; Dedhiya, M.; Plakogiannis, F.M. The effect of permeation enhancers on the viscosity and the release profile of transdermal hydroxypropyl methylcellulose gel formulations containing diltiazem HCl. *Drug Dev. Ind. Pharm*., **2010**, *36*(10), 1195-206.

[54] Simpson, D.; Noble, S.; Goa, K.L. Perindopril: In congestive heart failure. *Drugs*, **2002**, *62*(9), 1367-13677; discussion 1378-1379.

[55] Kute, A.; Goudanavar, P.; Hiremath, D.; Reddy, S.R. Development and characterization of perindopril erbumine loaded proniosomal gel. *Asian J. Pharm. Tech*., **2012**, *2*(2), 54-58.

[56] Yamamoto, S.; Karashima, M.; Arai, Y.; Tohyama, K.; Amano, N. Prediction of human pharmacokinetic profile after transdermal drug application using excised human skin. *J. Pharm. Sci*., **2017**, *106*(9), 2787-2794.

[57] Hayton, W.L.; Chen, T. Correction of perfusate concentration for sample removal. *J. Pharm. Sci*., **1982**, *71*(7), 820-821.

[58] Friend, D.R. *In vitro* skin permeation techniques. *J. Control. Release*, **1992**, *18*(3), 235-248.

[59] Ita, K.B.; Du Preez, J.; Lane, M.E.; Hadgraft, J.; du Plessis, J. Dermal delivery of selected hydrophilic drugs from elastic liposomes: Effect of phospholipid formulation and surfactants. *J. Pharm. Pharmacol*., **2007**, *59*(9), 1215-1222.

[60] Hathout, R.M.; Woodman, T.J.; Mansour, S.; Mortada, N.D.; Geneidi, A.S.; Guy, R.H. Microemulsion formulations for the transdermal delivery of testosterone. *Eur. J. Pharm. Sci.*, **2010**, *40*(3), 188-196.

[61] Sekkat, N.; Kalia, Y.N.; Guy, R.H. Porcine ear skin as a model for the assessment of transdermal drug delivery to premature neonates. *Pharm. Res*., **2004**, *21*(8), 1390-1397.

[62] Burger, C.; Gerber, M.; du Preez, J.L.; du Plessis, J. Optimised transdermal delivery of pravastatin. *Int. J. Pharm*., **2015**, *496*(2), 518-525.

[63] Meyer, W.; Kacza, J.; Zschemisch, N.H.; Godynicki, S.; Seeger, J. Observations on the actual structural conditions in the stratum superficiale dermidis of porcine ear skin, with special reference to its use as model for human skin. *Ann. Anat*., **2007**, *189*(2), 143-156.

[64] Silva, S.M.C.; Hu, L.; Sousa, J.J.S.; Pais, A.A.C.C.; Michniak-Kohn, B.B. A combination of nonionic surfactants and iontophoresis to enhance the transdermal drug delivery of ondansetron HCl and diltiazem HCl. *Eur. J. Pharm. Biopharm*., **2012**, *80*(3), 663-673.

[65] Gupta, R.; Mukherjee, B. Development and *in vitro* evaluation of diltiazem hydrochloride transdermal patches based on povidone-ethylcellulose matrices. *Drug Dev. Ind. Pharm*., **2003**, *29*(1), 1-7.

[66] Sarkar, G.; Saha, N.R.; Roy, I.; Bhattacharyya, A.; Bose, M.; Mishra, R.; Rana, D.; Bhattacharjee, D.; Chattopadhyay, D. Taro corms mucilage/HPMC based transdermal patch: An efficient device for delivery of diltiazem hydrochloride. *Int. J. Biol. Macromol*., **2014**, *66*, 158-165.

[67] Parhi, R.; Suresh, P. Transdermal delivery of Diltiazem HCl from matrix film: Effect of penetration enhancers and study of antihypertensive activity in rabbit model. *J. Adv. Res*., **2016**, *7*(3), 539-550.

[68] Anirudhan, T.S.; Nair, A.S.; Gopika, S.S. The role of biopolymer matrix films derived from carboxymethyl cellulose, sodium alginate and polyvinyl alcohol on the sustained transdermal release of diltiazem. *Int. J. Biol. Macromol*., **2018**, *107*(Pt A), 779-789.

[69] Monti, D.; Egiziano, E.; Burgalassi, S.; Chetoni, P.; Chiappe, C.; Sanzone, A.; Tampucci, S. Ionic liquids as potential enhancers for transdermal drug delivery. *Int. J. Pharm*., **2017**, *516*(1-2), 45-51.

[70] Bhunia, T.; Giri, A.; Nasim, T.; Chattopadhyay, D.; Bandyopadhyay, A. Uniquely different PVA-xanthan gum irradiated membranes as transdermal diltiazem delivery device. *Carbohydr. Polym*., **2013**, *95*(1), 252-261.

[71] Siepmann, J.; Peppas, N.A. Higuchi equation: Derivation, applications, use and misuse. *Int. J. Pharm*., **2011**, *418*(1), 6-12.

[72] Fu, Y.; Kao, W.J. Drug release kinetics and transport mechanisms of non-degradable and degradable polymeric delivery systems. *Expert Opin. Drug Deliv*., **2010**, *7*(4), 429-444.

[73] Masaro, L.; Zhu, X.X. Physical models of diffusion for polymer solutions, gels and solids. *Prog. Polym. Sci*., **1999**, *24*(5), 731-775.

[74] Mockel, J.E.; Lippold, B.C. Zero-order drug release from hydrocolloid matrices. *Pharm. Res*., **1993**, *10*(7), 1066-1070.

[75] Jain, S.K.; Chourasia, M.K.; Sabitha, M.; Jain, R.; Jain, A.K.; Ashawat, M.; Jha, A.K. Development and characterization of transdermal drug delivery systems for diltiazem hydrochloride. *Drug Deliv*., **2003**, *10*(3), 169-177.

[76] Remko, M.; Bojarska, J.; Ježko, P.; Maniukiewicz, W.; Olczak, A. Molecular structure of antihypertensive drug perindopril, its active metabolite perindoprilat and impurity F. *J. Mol. Struct.*, **2013**, *1036*, 292-297.

[77] Helal, F.; Lane, M.E. Transdermal delivery of Angiotensin Converting Enzyme inhibitors. *Eur. J. Pharm. Biopharm*., **2014**, *88*(1), 1-7.

[78] Kute, A.; Goundanavar, P.; Hiremath, D, Reddy, S.R. Development and characterization of perindopril erbumine proniosomal gel. *Asian J. Pharm. Tech*., **2012**, 54-58.

[79] Chen, M.C.; Ling, M.H.; Lai, K.Y.; Pramudityo, E. Chitosan microneedle patches for sustained transdermal delivery of macromolecules. *Biomacromolecules*, **2012**, *13*(12), 4022-4031.

[80] Olatunji, O.; Olsson, R.T. Microneedles from fishscale-nanocellulose blends using low temperature mechanical press method. *Pharmaceutics*, **2015**, *7*(4), 363-378.

[81] Pearton, M.; Kang, S.-M.; Song, J.-M.; Kim, Y.-C.; Quan, F.-S.; Anstey, A.; Ivory, M.; Prausnitz, M.R.; Compans, R.W.; Birchall, J.C. Influenza virus-like particles coated onto microneedles can elicit stimulatory effects on Langerhans cells in human skin. *Vaccine*, **2010**, *28*(37), 6104-6113.

[82] Badran, M.M.; Kuntsche, J.; Fahr, A. Skin penetration enhancement by a microneedle device (Dermaroller) *in vitro*: Dependency on needle size and applied formulation. *Eur. J. Pharm. Sci*., **2009**, *36*(4-5), 511-523.

[83] Wermeling, D.P.; Banks, S.L.; Hudson, D.A.; Gill, H.S.; Gupta, J.; Prausnitz, M.R.; Stinchcomb, A.L. Microneedles permit transdermal delivery of a skin-impermeant medication to humans. *Proc. Natl. Acad. Sci. U.S.A*., **2008**, *105*(6), 2058-2063.

[84] Mönkäre, J.; Reza Nejadnik, M.; Baccouche, K.; Romeijn, S.; Jiskoot, W.; Bouwstra, J.A. IgG-loaded hyaluronan-based dissolving microneedles for intradermal protein delivery. *J. Control. Release*, **2015**, *218*, 53-62.

[85] Kaur, M.; Ita, K.B.; Popova, I.E.; Parikh, S.J.; Bair, D.A. Microneedle-assisted delivery of verapamil hydrochloride and amlodipine besylate. *Eur. J. Pharm. Biopharm*., **2014**, *86*(2), 284-291.

[86] Li, G.; Badkar, A.; Nema, S.; Kolli, C.S.; Banga, A.K. *In vitro* transdermal delivery of therapeutic antibodies using maltose microneedles. *Int. J. Pharm*., **2009**, *368*(1-2), 109-115.

[87] Devraj; Bhatt, D.C.; Mohd, A. A review: Different generation approaches of transdermal drug delivery System. *J. Chem. Pharm. Res*., **2010**, *2*, 184-193.

[88] Barry, B.W. Novel mechanisms and devices to enable successful transdermal drug delivery. *Eur. J. Pharm. Sci*., **2001**, *14*(2), 101-114.

[89] Nguyen, J.; Ita, K.B.; Morra, M.J. Popova IETransdermal delivery of carbamazepine and tiagabine hydrochloride. *Pharmaceutics*, **2016**, *8*(4), pii: E33.